

Baroclinic anomalies associated with the Southern Hemisphere Annular Mode: Roles of synoptic and low-frequency eddies

Yu Nie,¹ Yang Zhang,¹ Xiu-Qun Yang,¹ and Gang Chen²

Received 13 February 2013; revised 18 March 2013; accepted 21 March 2013; published 29 May 2013.

[1] Using the ERA-40 reanalysis data, we study the different roles of synoptic and low-frequency eddies in sustaining the latitudinal shift of the low-level baroclinicity associated with the Southern Hemisphere Annular Mode. The eddy effect is assessed through the direct eddy thermal forcing via eddy heat flux and the indirect forcing via eddy-driven mean meridional circulation (MMC). We find that in addition to the synoptic eddy-induced MMC suggested by Robinson (2006), the direct eddy thermal forcing by low-frequency eddies is significant in driving the baroclinic anomalies. These two processes together prevail over the direct baroclinicity deduction by synoptic eddies. The different effects of synoptic and low-frequency eddies might be attributed to the distinct latitudinal distributions of their low-level eddy heat flux relative to the midlatitude jet. The different roles of the MMC induced by synoptic eddy momentum and heat flux are also emphasized, with the former leading the baroclinic anomalies and the latter acting to extend the baroclinic anomalies. **Citation:** Nie, Y., Y. Zhang, X.-Q. Yang, and G. Chen (2013), Baroclinic anomalies associated with the Southern Hemisphere Annular Mode: Roles of synoptic and low-frequency eddies, *Geophys. Res. Lett.*, 40, 2361–2366, doi:10.1002/grl.50396.

1. Introduction

[2] As the leading mode of Southern Hemisphere extratropical variability on intraseasonal time scales, the Southern Hemisphere Annular Mode (SAM) exhibits an equivalent barotropic dipolar pattern and is often described as a nearly zonally symmetric latitudinal displacement of the midlatitude jet [Hartmann and Lo, 1998; Thompson and Wallace, 2000]. As an internal mode of variability, understanding the mechanisms sustaining the persistence of the SAM will be important for intraseasonal forecasting and predicting circulation change under a changing climate.

[3] The observational study by Lorenz and Hartmann [2001] suggested that the persistence of the SAM is a consequence of a positive feedback between the synoptic (high-frequency) eddy momentum forcing and the zonal flow, and a poleward displacement of the jet is often followed by a poleward shift of the maximum low-level baroclinic zone where the eddy generation is strongest [Kidston *et al.*,

2010]. Robinson [2000] argued that this latitudinal shift of baroclinicity may prolong the time scale of the SAM through a positive feedback loop: the baroclinicity shift results in the latitudinal shift of the eddy generation, which further causes a shift of the eddy momentum flux aloft and then extends the zonal wind anomaly. Thus, the latitudinal shift of the low-level baroclinicity could be crucial for extending the persistence of the SAM [Robinson, 2006; Chen and Plumb, 2009; Zhang *et al.*, 2012].

[4] In previous theoretical studies, different dynamical processes have been proposed for sustaining the baroclinic anomalies in the annular modes. Robinson [2006] suggested that the upper level eddy momentum convergence, as shown in Figure 1a, by driving a thermally indirect mean meridional circulation (MMC), may reinforce the low-level baroclinicity displacement. This mechanism is also discussed in Gerber and Vallis [2007] and Hartmann [2007]. The recent work by Zhang *et al.* [2012] emphasized the role played by low-frequency eddies. As shown in Figure 1b, because the low-frequency eddy generation is located at the jet flank, its direct thermal forcing can locally enhance the low-level baroclinicity at the jet center, which acts to reinforce the baroclinic anomalies in the annular modes. The work also proposed a baroclinic mechanism in which the synoptic and low-frequency eddies work together maintaining the positive feedback in the annular modes. That is, following the anomalous zonal wind and the associated critical line variations, the anomalous low-frequency eddy thermal forcing drives a latitudinal shift of the lower level baroclinic zone, which results in a latitudinal displacement of the synoptic eddy generation. The anomalous synoptic eddy momentum forcing aloft further enhances the zonal wind anomalies. Hence, synoptic and low-frequency eddies can play different roles in sustaining the annular modes.

[5] In this study, by explicitly diagnosing the eddy-induced MMC, different dynamical processes suggested in Robinson [2006] and Zhang *et al.* [2012] will be examined, and how the synoptic and low-frequency eddies work together in sustaining the baroclinic anomalies in the SAM will be investigated. Using the reanalysis data, we will show the importance of the low-frequency eddy thermal forcing and the synoptic eddy-induced MMC forcing for shifting the low-level baroclinicity. Furthermore, the different roles played by the MMC induced by synoptic eddy momentum and heat flux in sustaining the baroclinic anomalies are also emphasized. Our work also indicates that the different roles played by synoptic and low-frequency eddies in the SAM might be related to the distinct latitudinal distributions of their eddy heat flux relative to the midlatitude jet.

[6] The structure of this paper is arranged as follows. Data set and analysis methods used in the study are described in section 2. Baroclinic anomalies associated with SAM are

¹Institute for Climate and Global Change Research, School of Atmospheric Sciences, Nanjing University, Nanjing, China.

²Department of Earth and Atmospheric Sciences, Cornell University, Ithaca, New York, USA.

Corresponding author: Y. Zhang, School of Atmospheric Sciences, Nanjing University, 22 Hankou Rd., Nanjing, Jiangsu, 210093, China. (yangzh@alum.mit.edu)

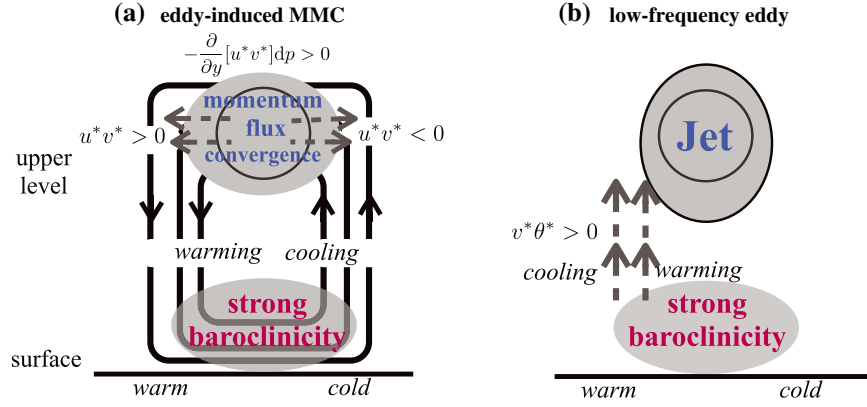


Figure 1. Schematics illustrating the mechanisms through which (a) the eddy-induced MMC suggested by *Robinson* [2006] and (b) the low-frequency eddies suggested by *Zhang et al.* [2012] act to enhance the low-level baroclinicity. Dashed arrows denote the propagation of eddy activity.

studied in section 3, in which variations of the low-level baroclinicity with SAM and the different roles of synoptic and low frequency eddies in sustaining the baroclinic anomalies are investigated. Summary and discussions are presented in section 4.

2. Data and Methodology

2.1. Data Analysis

[7] For this study, we use 44 year (1958–2001) European Center for Medium-Range Weather Forecasts reanalysis (ERA-40) daily (1200 UTC) wind and temperature data at constant pressure levels [Uppala *et al.*, 2005]. The analyses shown in this work were also tested using the corresponding National Centers for Environmental Prediction-National Center for Atmospheric Research reanalysis data [Kalnay *et al.*, 1996] to guarantee the consistence of the results. Following *Lorenz and Hartmann* [2001], we analyze the full year daily anomaly data for the Southern Hemisphere. The daily anomaly is computed by removing the mean seasonal cycle, and the mean seasonal cycle is defined as the annual average plus the first four Fourier harmonics of the 44 year daily climatology. We perform empirical orthogonal function (EOF) analyses on the daily anomalous zonal flow from 30°S to 70°S. For the EOF analysis, the data fields are properly weighted by the square root of the cosine of latitude [North *et al.*, 1982] to account for the decrease of area toward the pole.

[8] To compute the time-filtered eddy fluxes, we first use a 10 day high- and low-pass Lanczos filter [Emery and Thomson, 2001] to divide the eddy component of zonal wind, u^* ; meridional wind, v^* ; and temperature, T^* , into high- and low-frequency parts: u_h^* , v_h^* , T_h^* , and u_l^* , v_l^* , T_l^* . Then, the eddy fluxes are divided into three parts as in *Lorenz and Hartmann* [2001]: the eddy fluxes by high-frequency eddies [$u_h^*v_h^*$], [$v_h^*T_h^*$]; the eddy fluxes by low-frequency eddies [$u_l^*v_l^*$], [$v_l^*T_l^*$]; and the eddy fluxes by cross-frequency eddies [$u_h^*v_l^* + u_l^*v_h^*$], [$v_h^*T_l^* + v_l^*T_h^*$]. For the spacial filtering, we use a fast Fourier transformation to partition the eddy fluxes into individual zonal wave number. Space-time co-spectra analyses are applied to characterize the distributions of high- and low-frequency eddies that contribute to the zonal mean eddy heat fluxes [Randel and Held, 1991; Kim and Lee, 2004]. For the spectra analysis, the input time series are divided into 256 day long segments, with

128 days overlapping between them. Thus, for the 44 year long data, this gives over 100 spectra realizations for the composite spectrum.

2.2. Diagnosing Eddy-Induced MMC

[9] From the meridional derivative of the zonal mean thermodynamic equation under quasi-geostrophic approximation,

$$\frac{\partial}{\partial t} \left(-\frac{\partial}{\partial y} [T] \right) = \frac{\partial^2}{\partial y^2} [v^* T^*] - \frac{\partial}{\partial y} \Gamma [\omega] - \mathcal{R}, \quad (1)$$

where $\Gamma = -T \partial \ln \theta / \partial p$ is a static stability parameter; the variation of the zonal mean baroclinicity ($-\partial [T] / \partial y$) is driven by three components: the direct eddy thermal forcing via eddy heat flux, the adiabatic heating/cooling through MMC and \mathcal{R} , the diabatic heating. In extratropics, MMC is strongly driven by eddy fluxes, though as suggested in *Feldstein* [2001], surface friction and diabatic heating could also play a role. Thus, both the direct eddy thermal forcing and the eddy-induced MMC forcing should be evaluated as the eddy effects on the baroclinicity, which are also the two important dynamical processes suggested by previous studies.

[10] In this study, the MMC induced by anomalous eddy momentum and heat fluxes associated with SAM is diagnosed explicitly by solving the zonally symmetric quasi-geostrophic omega equation as in *Haynes and Shepherd* [1989]:

$$L\omega(p, \mu) = \frac{2\Omega a p}{R\Gamma} \frac{\partial}{\partial \mu} \left[\frac{(1-\mu^2)^{1/2}}{\mu} \frac{\partial F}{\partial p} \right] - \Gamma^{-1} \frac{\partial}{\partial \mu} \left[\frac{(1-\mu^2)}{\mu^2} \frac{\partial Q}{\partial \mu} \right], \quad (2)$$

where

$$L = \frac{\partial}{\partial \mu} \left[\frac{1-\mu^2}{\mu^2} \frac{\partial}{\partial \mu} \right] + \frac{4\Omega^2 a^2 p}{R\Gamma} \frac{\partial^2}{\partial p^2}, \quad (3)$$

$\mu = \sin(\phi)$, ϕ is latitude. F and Q are, respectively, the momentum and thermal forcing terms. Here only the eddy sources of the F and Q are considered, where

$$F = -\frac{1}{a(1-\mu^2)^{1/2}} \frac{\partial \{ (1-\mu^2) [u^* v^*] \}}{\partial \mu}, \quad (4)$$

$$Q = -\frac{1}{a} \frac{\partial \{ (1-\mu^2)^{1/2} [v^* T^*] \}}{\partial \mu}. \quad (5)$$

The boundary conditions, same as in *Haynes and Shepherd* [1989], are taken to be $v = 0$ at the poles, $\omega = 0$ at $p = 0$,

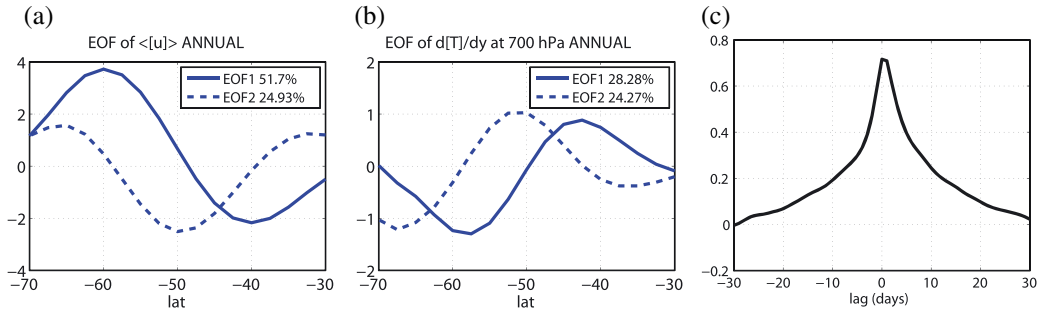


Figure 2. (a) Leading EOFs of zonal wind $\langle [u] \rangle$. (b) First two EOFs of zonal mean meridional temperature gradient at 700 hPa. (c) Lagged correlation between PC1 of 700 hPa meridional temperature gradient and UPC1. Positive lags denote that zonal wind leads.

and $D\Phi/Dt = 0$ at the lower surface $p = 1000$ hPa, where Φ is the geopotential. This lower boundary condition takes into account the effect of surface pressure variation. Equation (2) is solved by expanding onto the Hough functions, same as the method in Plumb [1982], Haynes and Shepherd [1989], and Feldstein [2001]. This new analysis allows us to attribute the changes in MMC to different eddy forcings.

[11] Furthermore, as described in section 2.1, eddy momentum and heat fluxes are all further divided into three parts: forcings by high-, low-, and cross-frequency eddies. Correspondingly, ω induced by these eddy momentum and thermal forcings can be calculated individually by solving the omega equation and be denoted by ω_F^h , ω_F^l , ω_F^{cross} , and ω_Q^h , ω_Q^l , ω_Q^{cross} , respectively. Thus, each component in the eddy forcing via eddy-induced MMC on the baroclinic anomalies can be diagnosed and compared to the direct thermal forcing. All mechanisms suggested by Robinson [2006] and Zhang *et al.* [2012] can be examined explicitly in this study.

3. Results

3.1. Baroclinic Anomalies Associated With SAM

[12] To investigate the relationship between the anomalous zonal wind in the SAM and the lower level baroclinicity, time series of the anomalous zonal wind and baroclinicity are calculated. An EOF analysis is applied to the extratropical (30°S – 70°S) anomalous zonal wind. To distinguish from the baroclinic component, as in Lorenz and Hartmann [2001], the vertically integrated zonal mean zonal wind is used for the analysis. The first two EOFs are shown in Figure 2a. The leading mode represents a latitudinal shift of the midlatitude jet. The principal component time series associated with the leading EOF hereafter is defined as UPC1. The second mode may be described as a strengthening or weakening of the jet intensity. As in Blanco-Fuentes and Zurita-Gotor [2011], we also perform an EOF analysis on 700 hPa temperature meridional gradient to describe the variability of the low-level baroclinicity. The leading mode manifests a meridional displacement of baroclinicity about its mean position (Figure 2b), while the second mode represents a sharpening or broadening of the maximum baroclinicity. The results are similar for other low-level pressure levels (e.g., 850 hPa). The pattern of the leading mode is more significant and robust as we move to the lower frequencies (results not shown), which is consistent with the results in Blanco-Fuentes and Zurita-Gotor [2011]. A lagged correlation between UPC1 and PC1 of temperature meridional gradient at 700 hPa is then estimated. As shown in Figure 2c,

the correlation reaches its maximum at day 1, which indicates that the jet shift is followed by a shift of the low-level baroclinicity at small lags.

3.2. Roles of High- and Low-Frequency Eddies

[13] To investigate the roles of high- and low-frequency eddies that contribute to the baroclinic anomalies associated with SAM, we first calculate the covariance spectra of the 700 hPa eddy meridional heat flux, using the method in Randel and Held [1991]. Figure 3a shows the zonal wave number-phase speed co-spectra meridionally averaged over 40°S – 70°S , where the heat flux is strong. The corresponding zonal wave number-period co-spectra is plotted in Figure 3b. The eddy fluxes are dominated by eastward propagating disturbances from zonal wave numbers 1–8, with higher zonal wave number eddies moving at faster phase speeds and characterized with shorter time scales. Eddies from zonal wave numbers 5–8 are mainly characterized by synoptic time scales, around 2–8 days. Eddies from zonal wave numbers 1–4 have a broader range of periods, 10–30 days. Thus, in the following analyses, we partition the eddy fluxes into two groups: the contributions from zonal wave numbers 1–4 and 5–8, which can also approximately represent the contributions from respectively low- and high-frequency eddies.

[14] To test the mechanism suggested by Zhang *et al.* [2012], we further estimate the distributions of the 700 hPa eddy meridional heat fluxes from zonal wave numbers 1–4 and 5–8 as a function of latitude and phase speed. The 700 hPa zonal mean zonal wind is also plotted to denote the position of the midlatitude jet. As shown in Figure 3d, the heat fluxes from wave 5–8 are characterized by high-phase speed and peak near the jet center. For heat fluxes from wave 1–4, as in Figure 2c, they are characterized by lower phase speed, and, in contrast to the high-frequency eddies, they peak at the poleward flank of the jet. The magnitudes of the co-spectra also show that the eddy components from wave 1–4 are comparable to wave 5–8, which indicates that the effects of the low-frequency eddies cannot be ignored. Figures 3c and 3d also show that the locations where the two groups of eddies peak are also the regions where their phase speeds are close to the zonal mean zonal wind (the regions of the critical line for high/low-frequency eddies). The above results are consistent with the model results presented by Zhang *et al.* [2012] and indicate that the high- and low-frequency eddies can play different roles in sustaining the anomalous thermal fields in the annular modes.

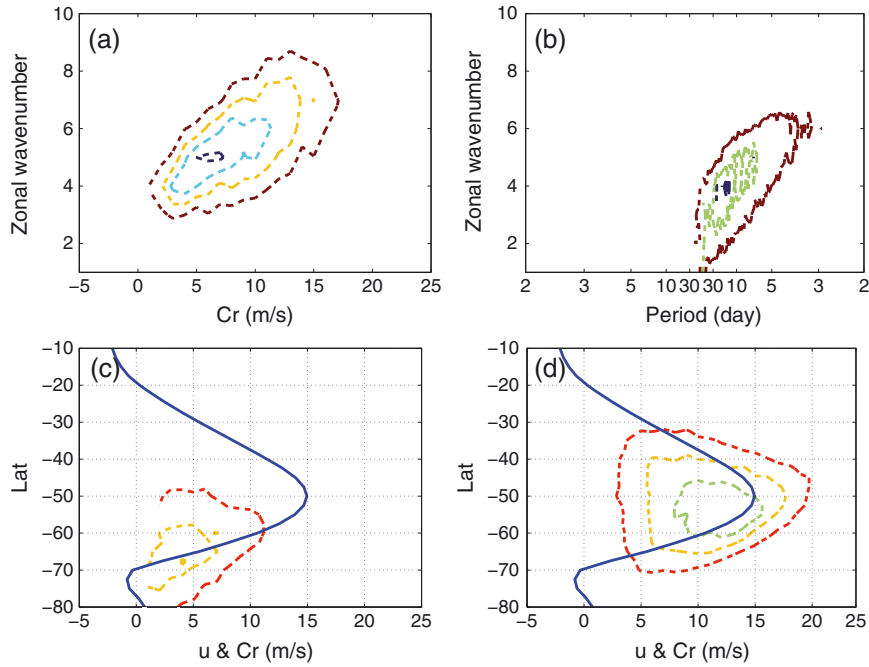


Figure 3. (a) Meridionally averaged (40°S – 70°S) zonal wave number-phase speed covariance spectra of $[v^*T^*]$ at 700 hPa. Contour interval is $0.01 \text{ K m s}^{-1} \Delta C_r^{-1}$, where the unit phase speed interval ΔC_r^{-1} is 1.0 m s^{-1} . (b) Zonal wave number-frequency (period) co-spectra of $[v^*T^*]$ of the same region. Spectral density contour interval is $0.001 \text{ K m s}^{-1} \Delta \varpi^{-1}$, with $\Delta \varpi$ the unit frequency interval of $(2\pi/256 \text{ days})$. Co-spectra of 700 hPa $[v^*T^*]$ as a function of zonal phase speed and latitude for zonal wave numbers (c) 1–4 and (d) 5–8. Contour interval is $0.05 \text{ K m s}^{-1} \Delta C_r^{-1}$. The blue solid line denotes the 700 hPa zonally averaged zonal wind.

3.2.1. Direct Eddy Thermal Forcing Versus Indirect Eddy-Induced MMC Forcing

[15] As described in section 2.2, the effect of high- and low-frequency eddies on the evolution of the baroclinic anomalies associated with SAM is evaluated through the direct eddy thermal forcing and the indirect eddy-induced MMC forcing. Figures 4a–4f show the lagged cross correlations between PC1 of low-level baroclinicity and the time series of each direct eddy forcing and indirect MMC forcing. The cross correlations for the net effect of the two forcings with PC1 are also estimated to compare their relative contributions. The forcing time series are calculated by projecting each component of the forcings (or the net effect of two forcings) onto the leading EOF mode of the baroclinicity at 700 hPa. The roles of the total direct eddy thermal forcing and eddy-induced MMC forcing in sustaining the baroclinic anomalies are shown in Figure 4a. The effect of the “observed” MMC on the baroclinic anomalies is also plotted, in which the vertical velocity from the reanalysis data is used. Its net effect with the direct eddy thermal forcing is estimated in Figure 4a as well, which is approximately equivalent to the effect of the transformed Eulerian mean residual circulation discussed in *Robinson* [2006] and *Hartmann* [2007]. The contributions of direct eddy forcing and indirect MMC forcing by high- and low-frequency eddies are also estimated in Figures 4b and 4c, respectively. These results are summarized as follows.

[16] 1. As shown in Figure 4a, the direct eddy thermal forcing displays strong positive correlations at short negative lags, which suggests a strong driving effect on the latitudinal shift of the baroclinicity, and negative correlations at positive lags. The MMC forcing shows positive correlations

at both relatively long (i.e., larger than 5 days) positive and negative lags with weaker magnitudes. The lagged cross correlation for the observed MMC is similar to that of the eddy-induced MMC, but with slightly stronger positive correlations. This could be attributed to the fact that factors as surface friction also make contributions [*Robinson*, 1996, 2000].

[17] 2. For high-frequency eddies, its direct thermal forcing manifests a damping effect on the latitudinal shift of baroclinicity. The high-frequency eddy-induced MMC exhibits similar lagged correlations to that of the total eddy-induced MMC in Figure 4a, indicating its dominant role in driving a thermally indirect MMC to enhance the baroclinic anomalies.

[18] 3. Comparing Figure 4c with Figures 4a and 4b, we find that at short negative lags, it is the low-frequency eddy thermal forcing that most strongly leads and drives the shift of the baroclinicity, whose positive correlation is evidently stronger than that of the MMC driven by high-frequency eddies. At long positive lags, the latter is shown playing a dominant role extending the baroclinic anomalies as suggested by *Robinson* [2006], though the low-frequency eddy shows a minor contribution as well. The MMC forcing induced by low-frequency eddies acts to damp the shift.

[19] 4. Figure 4b also shows that for high-frequency eddies, the damping effect of its direct thermal forcing is strongest at short positive lags. This, combined with the low-frequency eddy behavior, is consistent with the baroclinic mechanism proposed by *Zhang et al.* [2012], that is, the latitudinal shift of the low-frequency eddy thermal forcing drives a latitudinal displacement of the low-level baroclinic zone. This can result in a latitudinal shift of the synoptic

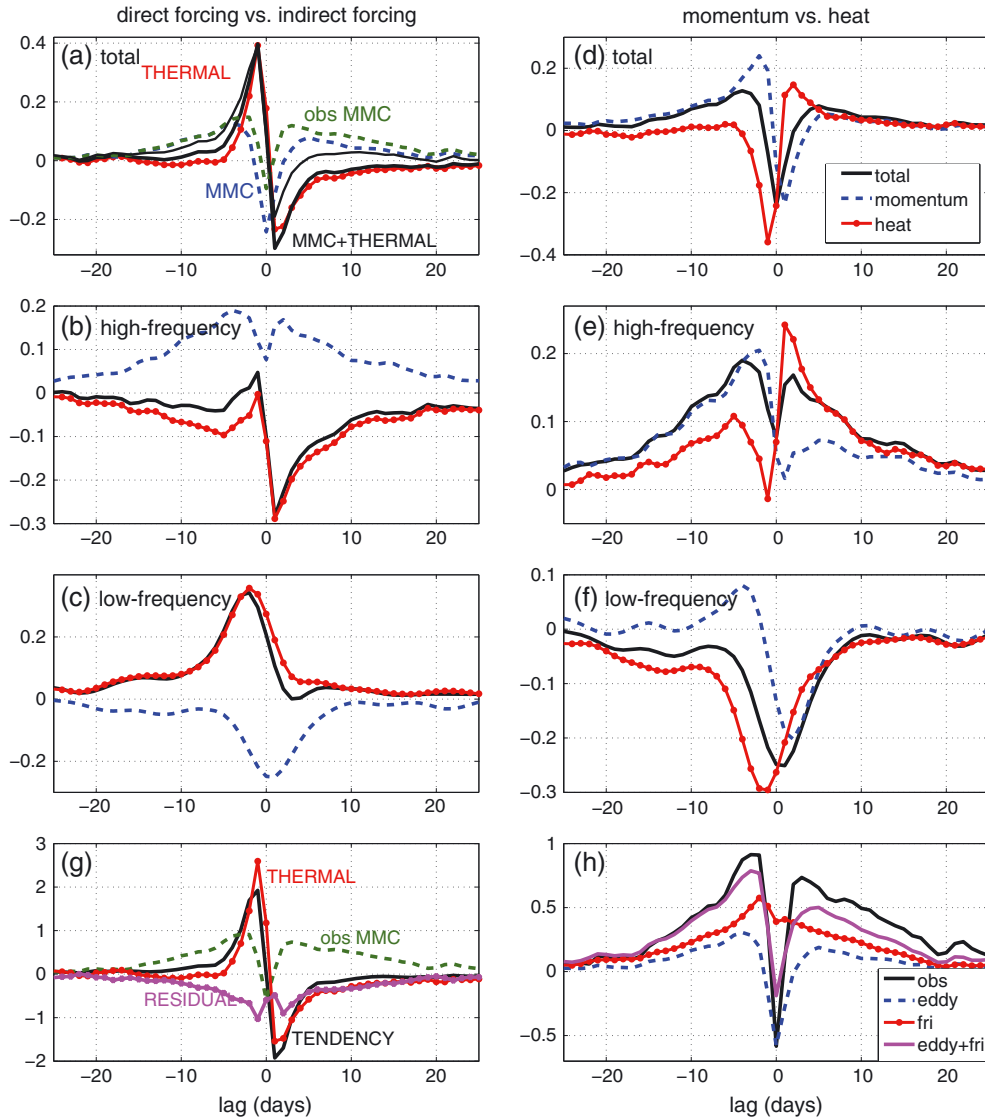


Figure 4. Lagged correlations between PC1 of zonal mean baroclinicity at 700 hPa and time series from the direct eddy thermal forcing, indirect eddy-induced MMC forcing, and the sum of the two by (a) total, (b) high-, and (c) low-frequency eddies, and forcing time series from the MMC driven by (d) total, (e) high-, and (f) low-frequency eddy momentum flux, heat flux, and eddy momentum + heat flux together. In Figure 4a, lagged correlations for the observed MMC forcing (green dashed curve) and its net effect with the eddy thermal forcing (thin black solid curve) are also plotted. Lagged covariance between zonal mean baroclinicity and (g) its main forcings, and the (h) forcings of the observed MMC, the MMC driven by eddy, friction, and the two together (Unit: $(\text{K}/1000 \text{ km})^2/\text{day}$). Positive lags denote that baroclinicity leads.

eddy generation, whose direct thermal effect would be a deduction of baroclinic anomalies.

[20] For the direct and indirect forcings from the cross-frequency eddies, their effects on the evolution of baroclinic anomalies are weak, whose results are thus not displayed here.

3.2.2. Eddy-Induced MMC: Momentum Flux Versus Heat Flux

[21] As in equation (2), the eddy-induced MMC can be further divided into the part driven by eddy momentum flux and the part driven by eddy heat flux, whose effects on the low-level baroclinicity variability are further investigated in Figures 4d–4f. These two parts of the MMC forcings are found playing different roles. As in Figure 4d, the MMC driven by total eddy momentum flux manifests a positive

peak at negative lags, but negative correlations at positive lags. The MMC driven by total eddy heat flux manifests almost opposite correlations. Figure 4e shows that at negative lags, the positive correlation in Figure 4d is mostly the contribution from the MMC driven by the momentum flux of high-frequency eddies, which indicates a driving effect on the baroclinicity shift. At positive lags, it mainly the MMC induced by the high-frequency eddy heat flux that acts to enhance and extend the baroclinic anomalies. For the MMC driven by low-frequency eddies, as shown in Figure 4f, the heat flux driven part damps the baroclinic anomalies strongest around short negative lags. The momentum flux-driven part shows slightly positive correlation at negative lags but damps the baroclinic anomalies evidently at positive lags.

[22] To confirm the above results, the correlation analyses are repeated by partitioning the eddies into zonal wave numbers 1–4 and 5–8 to approximate the low- and high-frequency eddies, respectively. The analyses show similar results, implying that our conclusions are robust and not sensitive to the filter we used. Due to space limit, these results are not shown here.

3.3. Discussion on the Roles of Other Factors

[23] In addition to high- and low-frequency eddies, there are other factors such as diabatic heating and surface friction also suggested to affect the baroclinic anomalies associated with SAM, whose effects will be qualitatively discussed in this section. The diabatic heating is estimated as the residual of equation (1), though this will include other smaller forcings from vertical eddy heat flux and horizontal advection of MMC. Figure 4g shows the covariance between the time series of forcing terms in equation (1) and PC1 of the baroclinicity. Compared with the direct eddy thermal forcing and the MMC forcing, diabatic heating plays a secondary role and always acts as a damping in the evolution of baroclinic anomalies. Surface friction, though not a direct forcing, can play an indirect role in the baroclinicity variation by affecting the MMC. Thus, here we estimate the frictional forcing as a residual from the momentum equation as in *Blanco-Fuentes and Zurita-Gotor* [2011], then calculate the friction-induced MMC by solving equation (2), the effect of which on the baroclinic anomalies is estimated and compared with the eddy-induced MMC (also observed MMC) in Figure 4h. The friction-induced MMC is found always acting to enhance the baroclinic anomalies. Its contribution is comparable to the eddy-induced MMC. As suggested by *Robinson*, [1996, 2000], surface friction, through the friction-induced MMC, is another important factor extending the baroclinic anomalies associated with SAM.

4. Summary and Discussion

[24] Using the ERA-40 reanalysis data, this study examines the different roles of synoptic and low-frequency eddies in sustaining the baroclinic anomalies associated with SAM. The latitudinal shift of the jet is followed by a latitudinal displacement of the low-level baroclinicity. In this study, we managed to explicitly diagnose the eddy-induced MMC to compare with the direct eddy thermal forcing, and we show that both the mechanisms proposed by *Robinson* [2006] and *Zhang et al.* [2012] work in the low-level baroclinicity restoration associated with SAM. The eddy thermal forcing by low-frequency eddies shows the strongest positive correlation leading the latitudinal shift of the baroclinicity. The high-frequency eddy-induced MMC plays a significant role enhancing and extending the lower level baroclinicity anomalies in the SAM. Furthermore, we emphasize the different roles played by the MMC induced by eddy momentum and heat fluxes in sustaining the baroclinic anomalies, with the former primarily driving the shift of the low-level baroclinicity and the latter mainly acting to extend the shift. We also argue that the different roles played by synoptic and low-frequency eddies in SAM might be attributed to the distinct meridional distribution of their eddy heat flux relative to the midlatitude jet, as suggested in *Zhang et al.* [2012].

[25] It is important to note that in this study, the indirect eddy forcing through the eddy-induced MMC was obtained from the omega equation under the quasi-geostrophic approximation, thus the results of this study could be qualitative. However, we anticipate that these qualitative results would be helpful in understanding the determining process of the variation of baroclinic anomalies. Work in progress is aimed at studying the dynamical explanation of the relationship between the high- and low-frequency eddies and understanding the annular modes under different mean states (i.e., the emergence of subtropical jet in the winter season, the poleward shift of the jet latitudes under global warming).

[26] **Acknowledgments.** We thank Alan Plumb for his help on solving the omega equation and two anonymous reviewers for their constructive suggestions. This study was supported by the National Natural Science Foundation of China under grant 41005028, 41275058, and the National Public Benefit Research Foundation of China under grant GYHY200806004. GC is supported by the US NSF award AGS-1248201.

[27] The Editor thanks two anonymous reviewers for their assistance in evaluating this paper.

References

- Blanco-Fuentes, J., and P. Zurita-Gotor (2011), The driving of baroclinic anomalies at different time scales, *Geophys. Res. Lett.*, *38*, L23805, doi: 10.1029/2011GL049785.
- Chen, G., and R. Plumb (2009), Quantifying the eddy feedback and the persistence of the zonal index in an idealized atmospheric model, *J. Atmos. Sci.*, *66*(12), 3707–3720.
- Emery, W. J., and R. E. Thomson (2001), *Data Analysis Methods in Physical Oceanography*, 2nd ed., 638 pp, Elsevier Science, Amsterdam.
- Feldstein, S. (2001), Friction torque dynamics associated with intraseasonal length-of-day variability, *J. Atmos. Sci.*, *58*(19), 2942–2953.
- Gerber, E., and G. Vallis (2007), Eddy-zonal flow interactions and the persistence of the zonal index, *J. Atmos. Sci.*, *64*(9), 3296–3311.
- Hartmann, D. (2007), The atmospheric general circulation and its variability, *J. Meteor. Soc. Japan*, *85*, 123–143.
- Hartmann, D., and F. Lo (1998), Wave-driven zonal flow vacillation in the Southern Hemisphere, *J. Atmos. Sci.*, *55*(8), 1303–1315.
- Haynes, P., and T. Shepherd (1989), The importance of surface pressure changes in the response of the atmosphere to zonally-symmetric thermal and mechanical forcing, *Quart. J. Roy. Meteor. Soc.*, *115*(490), 1181–1208.
- Kalnay, E., et al. (1996), The NCEP/NCAR 40-year reanalysis project, *Bull. Amer. Meteor. Soc.*, *77*(3), 437–471.
- Kidston, J., D. M. W. Frierson, J. A. Renwick, and G. K. Vallis (2010), Observations, simulations, and dynamics of jet stream variability and annular modes, *J. Climate*, *23*, 6186–6199.
- Kim, H., and S. Lee (2004), The wave-zonal mean flow interaction in the Southern Hemisphere, *J. Atmos. Sci.*, *61*(9), 1055–1067.
- Lorenz, D., and D. Hartmann (2001), Eddy-zonal flow feedback in the Southern Hemisphere, *J. Atmos. Sci.*, *58*(21), 3312–3327.
- North, G., F. Moeng, T. Bell, and R. Cahalan (1982), The latitude dependence of the variance of zonally averaged quantities, *Mon. Wea. Rev.*, *110*, 319–326.
- Plumb, R. A. (1982), Zonally symmetric hough modes and meridional circulations in the middle atmosphere, *J. Atmos. Sci.*, *39*, 983–991.
- Randel, W. J., and I. M. Held (1991), Phase speed spectra of transient eddy fluxes and critical layer absorption, *J. Atmos. Sci.*, *48*, 688–697.
- Robinson, W. A. (1996), Does eddy feedback sustain variability in the zonal index? *J. Atmos. Sci.*, *53*, 3556–3569.
- Robinson, W. A. (2000), A baroclinic mechanism for the eddy feedback on the zonal index, *J. Atmos. Sci.*, *57*, 415–422.
- Robinson, W. A. (2006), On the self-maintenance of midlatitude jets, *J. Atmos. Sci.*, *63*, 2109–2122.
- Thompson, D., and J. Wallace (2000), Annular modes in the extratropical circulation. Part I: Month-to-month variability, *J. Climate*, *13*(5), 1000–1016.
- Uppala, S. M., et al. (2005), The ERA-40 re-analysis, *Quart. J. Roy. Meteor. Soc.*, *131*, 2961–3012.
- Zhang, Y., X. Yang, Y. Nie, and G. Chen (2012), Annular mode like variation in a multi-layer QG model, *J. Atmos. Sci.*, *69*, 2940–2958.